Chemical Science

ROYAL SOCIETY OF CHEMISTRY

EDGE ARTICLE

View Article Online
View Journal | View Issue

Cite this: *Chem. Sci.*, 2022, **13**, 5846

All publication charges for this article have been paid for by the Royal Society of Chemistry

Received 15th February 2022
Accepted 28th March 2022

DOI: 10.1039/d2sc00952h

rsc.li/chemical-science

CPL on/off control of an assembled system by water soluble macrocyclic chiral sources with planar chirality†

Shixin Fa,[a] Takuya Tomita,[b] Keisuke Wada,[a] Kazuma Yasuhara,[cd] Shunsuke Ohtani,[a] Kenichi Kato,[a] Masayuki Gon,[e] Kazuo Tanaka,[e] Takahiro Kakuta,[b] Tada-aki Yamagishi[b] and Tomoki Ogoshi *[af]

Herein, we report the synthesis and planar chiral properties of a pair of water-soluble cationic pillar[5]arenes with stereogenic carbons. Interestingly, although units of the molecules were rotatable, only one planar chiral diastereomer existed in water in both cases. As a new type of chiral source, these molecules transmitted chiral information from the planar chiral cavities to the assembly of a water-soluble extended π-conjugated compound, affording circularly polarized luminescence (CPL). The chirality transfer process and resulting CPL were extremely sensitive to the feed ratio of the chiral pillar[5]arenes owing to the combined action of their planar chirality, bulkiness, and strong binding properties. When a limited amount of chiral source was added, further assembly of the extended π-conjugated compound into helical fibers with CPL was triggered. Unexpectedly, larger amounts of chiral source destroyed the helical fiber assemblies, resulting in elimination of the chirality and CPL properties from the assembled structures.

Introduction

Chirality is a widespread physical phenomenon in nature that is not only essential for various sophisticated biological activities, but has also been applied extensively in the field of materials science.[1] Among all research on chiral systems, functional materials with circularly polarized luminescence (CPL) have received extensive attention owing to their potential photonic applications, including sensors,[2] photoelectric devices,[3] chiroptical materials,[4] and 3D imaging.[5] In general, the fabrication of CPL materials can be achieved by two strategies. The first involves covalently connecting the chiral and fluorescent units to generate chiral luminescent small molecules[6] or polymers[7] and their assemblies.[8] This results in the two units being close together and enables the systems to possess relatively high dissymmetry values ($|g_{lum}|$). Extended π-conjugated moieties were widely present in such systems and successfully produced CPL materials with high $|g_{lum}|$.[9] In especial, pyrene moieties were frequently used as the fluorescent units.[10] Pyrene can show excimer fluorescence. It was demonstrated that the excimer of pyrene gave rise to higher CPL, promising CPL control by controlling the emission modes of pyrene derivatives. However, these systems sometimes suffer from cumbersome synthetic routes to introduce chiral units covalently. The other strategy uses the concept of chirality transfer to connect the chiral unit and fluorescent unit non-covalently and has produced various of successful CPL materials,[11] despite that the binding affinity of non-covalent bonds might turn to be low compared with covalent bonds.

Chiral macrocyclic molecules[12] with an intrinsic cavity might provide new candidates for a different mode of chirality transfer to fluorescent units owing to their bulky size, special chirality, and generally strong and specific host–guest complexing properties. This is promising for the fabrication of new supramolecular CPL materials.[13] However, this field remains underexplored owing to difficulties in the synthesis of chiral macrocycles and establishing effective chiral cavities. Only a few CPL materials based on host–guest interactions between fluorophores and cyclodextrins have been reported.[14] In

[a]*Department of Synthetic Chemistry and Biological Chemistry, Graduate School of Engineering, Kyoto University, Katsura, Nishikyo-ku, Kyoto 615-8510, Japan. E-mail: ogoshi@sbchem.kyoto-u.ac.jp*

[b]*Graduate School of Natural Science and Technology, Kanazawa University, Kakuma-machi, Kanazawa, Ishikawa, 920-1192, Japan*

[c]*Division of Materials Science, Graduate School of Science and Technology, Nara Institute of Science and Technology, 8916-5 Takayama, Ikoma, Nara 630-0192, Japan*

[d]*Center for Digital Green-innovation, Nara Institute of Science and Technology, 8916-5 Takayama, Ikoma, Nara 630-0192, Japan*

[e]*Department of Polymer Chemistry, Graduate School of Engineering, Kyoto University, Katsura, Nishikyo-ku, Kyoto 615-8510, Japan*

[f]*WPI Nano Life Science Institute (WPI-NanoLSI), Kanazawa University, Kakuma-machi, Kanazawa, Ishikawa, 920-1192, Japan*

† Electronic supplementary information (ESI) available: Chemicals, general methods, characterization, procedures and additional figures. See DOI: 10.1039/d2sc00952h

contrast to cyclodextrins, which have only one chirality, and most other macrocyclic molecules, which lack intrinsic chirality in general, pillar[*n*]arenes[15] are pillar-shaped macrocyclic hosts that exhibit planar chirality originating from the direction of substituents on their rims. These compounds possess two stable planar chiral isomers (*pR* and *pS*), and consequently produce two types of stable chiral cavity (Fig. 1).[16] These remarkable features have led to a few early-stage examples of CPL materials based on the single-molecule luminescence of functional pillar[*n*]arenes.[17]

Despite promising applications as supramolecular chiral sources, pillar[*n*]arenes with highly planar chiral purity have rarely been explored because flipping of their phenyl units leads to fast inversion of the planar chiral isomers.[18] Bulky groups on rims can inhibit the unit flip and generate two unconvertable enantiomers.[19] However, their isolation using chiral column chromatography is usually time-consuming and labor-intensive. Chiral control and regulation of pillar[5]arenes have also been performed by introducing stereogenic carbons onto their rims to form diastereomers.[20] However, the diastereomeric excess (de) was often low. Therefore, obtaining pillar[5]arenes with high planar chiral purity in a facile manner is among the most intriguing pillar[*n*]arene research areas. Herein, we report the first examples of cationic water-soluble planar chiral pillar[5]arenes with stereogenic carbons (*S*-**1** and *R*-**1** in Fig. 1), which were, unexpectedly, diastereomerically pure in water. By controlling the on/off transmission of planar chiral information from *S*-**1** and *R*-**1** to **APy**, a dendritic molecule fusing four linear alkyl acids with a π-conjugated core, using the feed amount of chiral pillar[5]arenes, CPL on/off-control of the assembly of **APy** was achieved. To our knowledge, this is the first example of a CPL on/off-control system dependent on the feed amount of the planar chiral sources.

Results and discussion

Synthesis, planar chiral properties, and host–guest properties of 1 in water

Synthesis of *S*-1 and *R*-1. Cationic water-soluble chiral pillar[5]arenes *S*-**1** and *R*-**1** (Fig. 1) were obtained by refluxing a solution of trimethylamine in ethanol with chiral pillar[5]arene precursors bearing 1-bromo-2-methylpropoxy groups on both rims (Scheme S1†). In principle, both *S*-**1** and *R*-**1** bearing ten stereogenic carbons on the rims possessed two stable planar chiral conformers, namely (*S*, *pS*)- and (*S*, *pR*)-conformers for *S*-**1**, and (*R*, *pS*)- and (*R*, *pR*)-conformers for *R*-**1**.

Solvent-dependent planar chiral expression of *S*-1 and *R*-1. The UV-vis spectra of **1** showed an absorption band at approx. 295 nm, which was attributed to π–π* transitions in the pillar[5]arene backbones (Fig. 2a and S1a†).[21] In the CD spectra, the positive Cotton effect in the π–π* transition region suggested the *pR*-rich planar chirality of *S*-**1** induced by the stereogenic carbon centers on the rims (Fig. 2a and S1b†).[22] Interestingly, the CD spectra of *S*-**1** were critically affected by the solvent employed. For example, the CD intensity of *S*-**1** in water was four times that in DMSO (Fig. S1b†). This indicated the unit-flip ability of *S*-**1**, meaning that conversion between the *pR* and *pS* planar chiral conformers of *S*-**1** could occur at room temperature.

^{1}H NMR spectra of *S*-**1** in aprotic solvents afforded two clear sets of resonance signals (Fig. 2b, S2 and S3†), indicating that *S*-**1** possessed both *pS* and *pR* conformations in these solvents.[23] For example, the de values of *S*-**1** in DMSO-d_6 and acetonitrile-d_3

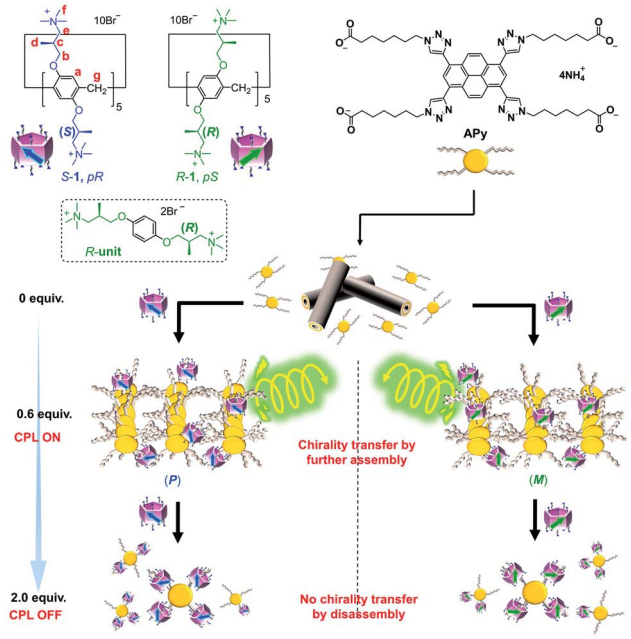

Fig. 1 Rational design of new supramolecular CPL on/off controllable materials using water-soluble planar chiral pillar[5]arenes *S*-**1** and *R*-**1**.

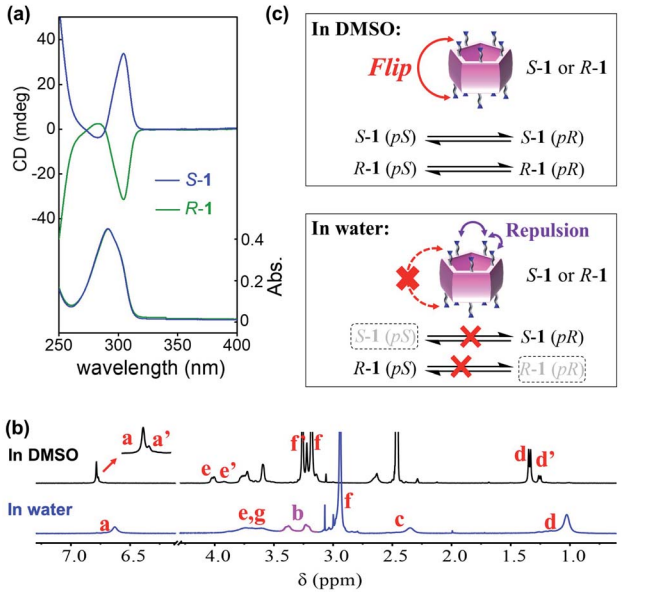

Fig. 2 (a) CD and UV-vis spectra of *S*-**1** and *R*-**1** (2×10^{-5} M) in water. (b) ^{1}H NMR spectra of *S*-**1** (400 MHz) in D_2O and DMSO-d_6. All spectra were recorded at 25 °C. (c) Illustration of the unit flip of *S*-**1** and *R*-**1** in DMSO and inhibition of the unit flip in water.

were determined to be approx. 60% and 26%, respectively. Unexpectedly, all protons on *S*-**1** showed only one set of resonance signals in D_2O (Fig. 2b).[24] Furthermore, the resonance signal of proton H_b in proximity to the pillar[5]arene core was split and hardly coalesced in D_2O, even at 80 °C (Fig. S5†), indicating that flipping of the pillar[5]arene units was inhibited or slow on the NMR timescale, and that interconversion between conformers was difficult in D_2O. Additionally, the dissymmetry value (g) of the induced CD intensity of *S*-**1** in water was 5.9×10^{-3} (Fig. S6†), which was around twice the g value of the previously reported water-soluble planar chiral pillar[5]arene with almost 100% diastereomeric purity,[25] and closer to those of enantiopure pillar[5]arenes in organic solvents (Table S1†).[19b,c,26] These observations implied that only the conformer with *pR* planar chirality ((*S*, *pR*)-conformer) existed in the aqueous solution of *S*-**1**. The CD spectra of *R*-**1** and *S*-**1** were mirror images (Fig. 2a), suggesting that *R*-**1** was diastereomerically pure in water with *pS* planar chirality (the (*R*, *pS*)-conformer).

The above results demonstrated that the bulkiness of the substituents on rims was turned out to be not enough to prevent the unit flip of the pillar[5]arenes, so the expression of planar chirality of *S*-**1** and *R*-**1** was critically affected by the solvent employed. Such solvent-dependent planar chiral expression was first caused by the solvation of the substituents on both rims. In water, the relatively strong repulsion between the hydrated trimethyl ammonium groups inhibited flipping of the pillar[5]arene units (Fig. 2c). In contrast, as an organic solvent, DMSO might not only fail to fully ionize the trimethylammoniums and their counter anions (Br^-), but also reduced the repulsion between the solvated trimethylammonium salts, which led to easier flipping of the pillar[5]arene units. In addition, the different orientations of substituents of **1** in different solvents also contributed to the solvent-dependent planar chiral expression according to our previous findings.[20a,23] There are two branches on each stereogenic carbon of **1**, one is the trimethylammonium, which is larger in polarity and volume, and the other is the methyl group, which is smaller in polarity and volume. In water, the branched methyl groups probably favored being located in the pillar[5]arene cavity, while the trimethylammoniums favored being outside due to hydration, leading to highly selective orientation of the side chains of **1**, which resulted in the high de value. Furthermore, this "open"-form with small groups inside and large groups outside often results in the *pR* chirality of *S*-**1** and *pS* chirality of *R*-**1**.[20a,23] In contrast, the difference in the location of the methyl branch and trimethylammonium branch decreased in aprotic solvent (such as DMSO), which further decreased the de value of **1**.

Host–guest properties of *S*-1 and *R*-1. Pillar[5]arenes with flippable units usually show low de values in solution.[20] The high planar chiral purity of *S*-**1** and *R*-**1** in water made them perfect candidates as chiral sources with effective chiral cavities that might show strong host–guest interactions with specific guest molecules.

Both *S*-**1** and *R*-**1** were able to form complexes with linear carboxylic acids **C4–C9** (Fig. 3 and S7–S15, and detailed discussion in the ESI†), because the pillar[5]arene cavity bound

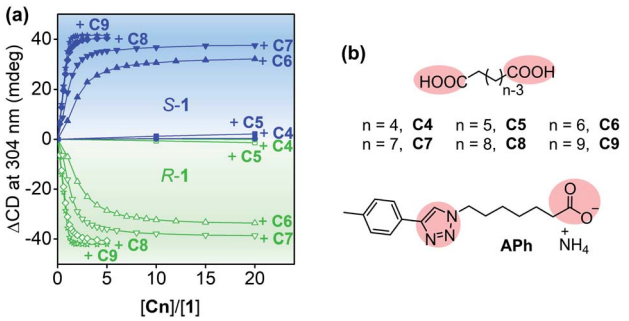

Fig. 3 (a) Plots of CD increase at 304 nm for *S*-**1** and *R*-**1** (2×10^{-5} M) upon addition of **C4–C9**. All spectra were recorded in water at 25 °C. (b) Molecular structures of **C4–C9** and **APh**.

the alkyl moieties *via* multiple C–H/π interactions,[27] and the trimethyl ammonium groups of **1** interacted with the acid groups of **C4–C9**.[28] The binding affinity increased significantly with increasing length of the guest molecules (Table S2†). For example, the association constants (K_a) of the complexes of *S*-**1** and *R*-**1** with **C8** reached 6.3×10^{-5} M^{-1} and 5.3×10^{-5} M^{-1}, respectively.

Chirality transfer on/off control from chiral 1 to APy in water

Molecular design and self-assembly of APy. Based on the binding properties of **1** in water, compound **APy** bearing four peripheral aliphatic acid chains and an extended π-conjugated core was synthesized (Fig. 1 and Scheme S3†). The aliphatic acid chains with the same linker as **C8** were expected to enable strong complexation between **APy** and **1**. The triazole moieties of **APy** also aid complexation according to previous reports.[29]

The assembly properties of **APy** in water due to π-oligomerization were initially investigated by concentration-variable fluorescence measurements (Fig. S16 and S17†). The critical assembly concentration (CAC) of **APy** was determined to be approx. 2×10^{-5} M in water, which was accordant with the concentration-dependent and temperature-variable ^{1}H NMR measurements (Fig. S18 and S19†).[30,31] All subsequent experiments were performed with an **APy** concentration of 6×10^{-5} M, which was higher than the CAC.

Two-step complexing process of Apy with 1. Complexation between **APy** and *S*-**1** was confirmed by ^{1}H NMR titration (Fig. S20†). Although the spectra were complicated, the signals corresponding to the linear alkyl chains of **APy** clearly showed dramatic upfield shift to around −1 to −2 ppm upon addition of *S*-**1**. This observation indicated the strong shielding effect resulting from the inclusion of these protons in the cavity of *S*-**1**. The binding mode and affinity between **APy** and *S*-**1** were estimated by investigating the binding between *S*-**1** and **APh** (Fig. 3b), which was the unit model of **APy** (Fig. S21–S24†). The association constant between *S*-**1** and **APh** was 8.0×10^5 M^{-1} (Fig. S24†), suggesting a strong binding.

Carefully examination of the ^{1}H NMR spectra of **APy** upon addition of *S*-**1** showed a two-step complexing process (Fig. S20†). With less than 0.6 equiv. of *S*-**1**, all resonance signals of **APy** underwent an upfield shift, while a gradual downfield

shift was observed with further addition of *S*-**1**. UV titration also suggested the same two-step process. In the aqueous solution, **APy** gave rise to absorption maxima at 253, 299, and 385 nm in a wide concentration range (Fig. S25†). The absorption band at approx. 385 nm decreased, broadened, and underwent a red-shift when less than 0.6 equiv. of planar chiral **1** was added, while adding more **1** resulted in the same band intensifying again (Fig. S26 and S27†).

Two-step chirality transfer from chiral 1 to Apy. As both *S*-**1** and *R*-**1** possess pure planar chirality in water, the chiral effect of **1** on **APy** was investigated (Fig. 4). Gratifyingly, both *S*-**1** and *R*-**1** induced the chirality in **APy**, as evidenced by the appearance of a CD signal at approx. 400 nm from the pyrene moiety upon addition of **1** (Fig. 4a). The CD signals indicated that *S*-**1** induced a positive Cotton effect on **APy**, while *R*-**1** induced a negative Cotton effect. Interestingly, the chiral induction ability of **1** exactly followed the trend of the two-step complexing process of **APy** (Fig. 4b and S28†), which was confirmed by ^{1}H NMR and UV titrations. Upon addition of less than 0.6 equiv. of chiral **1** to the aqueous solution of **APy**, the CD signals emerged gradually. Conversely, further addition of **1** caused a decrease in the chirality of **APy** previously acquired. When 2.0 equiv. of chiral **1** was added, the induced CD signals disappeared completely.

Such a two-step chiral induction process was beyond our expectation, because it behaved differently from most chirality transfer systems, where additional feeding of chiral sources usually improves the chirality transfer efficiency. As control experiments, the unit model of **1** (*R*-**unit** in Fig. 1) and l-valine methyl ester hydrochloride (L-**Val**) only caused a continuous decrease in the absorption at approx. 385 nm in the UV spectrum upon addition (Fig. S29†). Furthermore, these additives failed to transfer chirality to **APy**, even when added in large excess, except for causing random signals at approx. 400 nm that could be considered noise (Fig. S30 and S31†). These observations indicated that planar chiral **1** was effective compared with non-macrocyclic chiral sources and ensured successful two-step chirality transfer from the chiral source to **APy** in this system.

Transmission electron microscopy (TEM) images more clearly showed the effect of **1** on chirality transfer "on and off" control (Fig. 4c and S32†). Monolayered nanotubes of **APy** with a thickness of around 2.5 nm were changed to short bundle structures with partial helicity by adding 0.6 equiv. of chiral **1**, while further addition of **1** completely destroyed the assemblies of **APy** and only amorphous aggregates were observed.

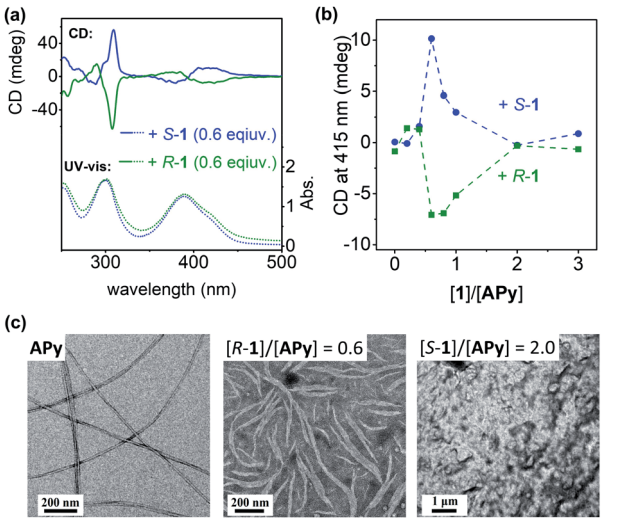

Fig. 4 (a) UV-vis and CD spectra of **APy** (6×10^{-5} M) with 0.6 equiv. of *S*-**1** and *R*-**1**. (b) Plots of CD at 415 nm for **APy** (6×10^{-5} M) upon addition of *S*-**1** and *R*-**1**. All spectra were recorded in water at 25 °C. (c) TEM images of **Apy** (left), and mixtures of **APy** with chiral **1** ([*R*-**1**]/[**APy**] = 0.6 (middle); [*S*-**1**]/[**APy**] = 2.0 (right)).

Mechanism of the two-step complexation and chirality transfer between chiral 1 and APy in water

To further clarify the two-step complexation and chirality transfer phenomena, the fluorescence change of **APy** caused by chiral **1** was investigated. On the fluorescence spectrum of **APy**, there are two emissions at approx. 426 nm and 531 nm (Fig. 5a), whose lifetimes were determined to be approx. 2.6 ns and 94 ns, respectively, which verified that the two emissions represented the monomeric **APy** and the excimer formed by stacking, respectively (Fig. S34†). Interestingly, upon adding chiral **1** to the aqueous solution of **APy**, a drastic spectral change was observed (Fig. 5a and S33†). Only 0.4 equiv. of *S*-**1** led to disappearance of the fluorescence band at approx. 426 nm and broadened the fluorescence band at approx. 531 nm (Fig. 5a). When *S*-**1** was further increased to 0.6 equiv., the emission maximum underwent a red-shift to approx. 545 nm, and the emission lifetime increased to 135 ns (Fig. S34†). The emission color gradually changed from light green to yellow during this process (Fig. 5b). These observations clearly suggested that *S*-**1** triggered oligomerization of **APy** through π–π stacking of extended pyrene moieties effectively. However, the emission at approx. 545 nm was gradually decreased and blue-shifted, accompanied by emergence of the band at approx. 426 nm upon addition of more than 0.6 equiv. of *S*-**1**. When 2.0 equiv. of *S*-**1** was added, the emission at approx. 545 nm disappeared and the emission color changed to blue, which indicated complete disassembly of **APy** to the monomeric state. The two-step complexation between **1** and **APy** were fast and efficient, as evidenced by that the fluorescent spectra of each titration were hardly changed within 9 hours at room temperature.

As shown in Fig. 5c, the neutralization of anions on **APy** by cations on **1** upon initial addition of **1** decreased repulsion between the molecules of **APy**, which had weakened the stacking of pyrene moieties, resulting in the assembly of **APy**. Theoretically, 0.4 equiv. of **1** possessed equal and opposite charges to **APy**. This was likely the reason for the monomeric emission disappearing in the fluorescence spectra of **APy** when 0.4 equiv. of **1** was added. A slight excess of **1** (0.6 equiv.) might regulate the assembly of **APy** and cause longer-range assembly. Taking advantage of the strong binding between **1** and **APy**, the assembly of **APy** obtained chiral information from planar chiral **1**. The CD signals shown in Fig. 4a indicated that *S*-**1** induced *P*-

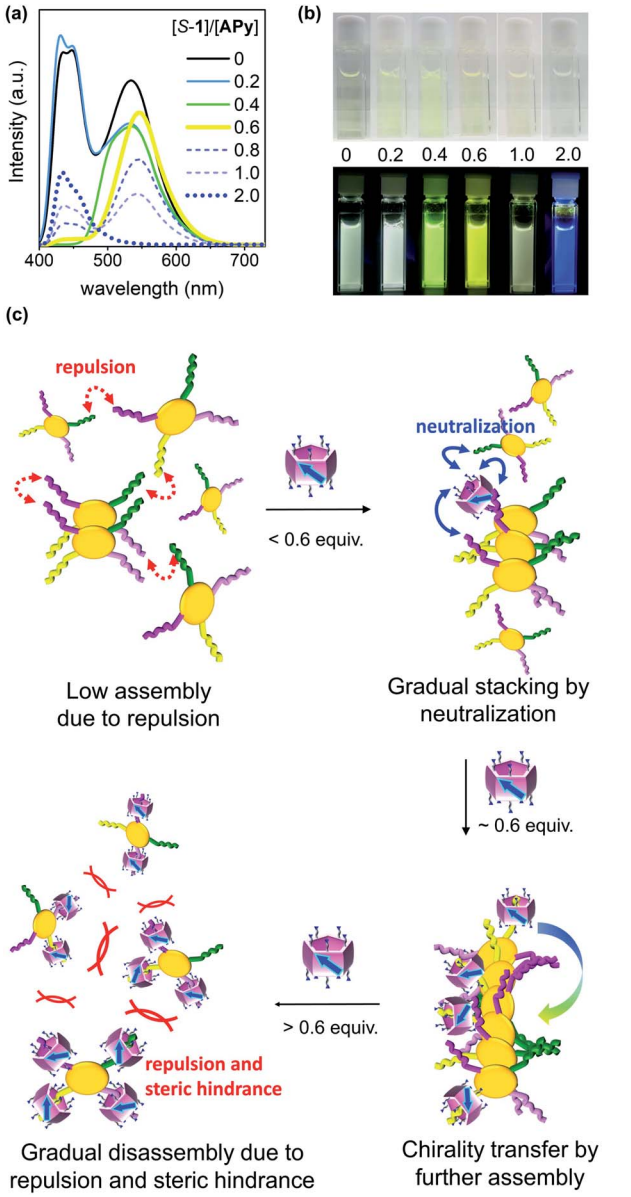

Fig. 5 (a) Fluorescence spectra ($\lambda_{ex} = 385$ nm) and (b) images of **APy** (6×10^{-5} M) upon addition of *S*-**1** under visible (top) and UV light (365 nm). All spectra were recorded in water at 25 °C. (c) Schematic illustration of the proposed two-step chirality transfer between *S*-**1** and **APy** upon changing the feed amount of *S*-**1**. The four peripheral chains of **APy** are shown in different colors for clarifying.

helicity in the assembly of **APy**, while *R*-**1** induced *M*-helicity. Further addition of **1** caused repulsion between the stable complex (**APy**·$\mathbf{1}_n$) owing to excess cations and steric hindrance between the bulky pillar[5]arenes, leading **APy** to depolymerize and the previously acquired chirality to gradually disappear.

CPL on/off control of the assembled system of APy by chiral 1 in water

The acquired helical assemblies of **APy** (6×10^{-5} M) possessed relatively strong fluorescence emission. For example, the quantum yields in the presence of 0.6 equiv. of *S*-**1** and *R*-**1** were

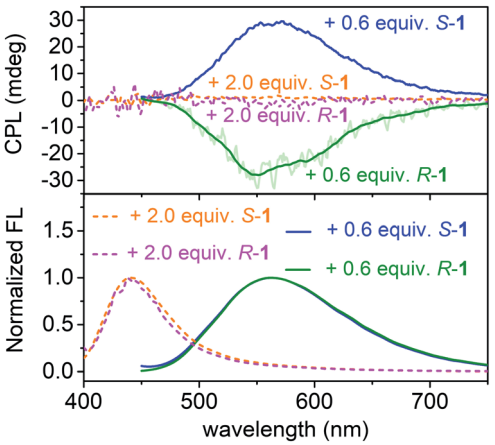

Fig. 6 CPL (top) and fluorescence (bottom) spectra of **Apy** (6×10^{-5} M) in the presence of 0.6 equiv. (solid lines) and 2.0 equiv. (dashed lines) of chiral **1**. All spectra were recorded in water at 25 °C.

0.43 and 0.47, respectively (Table S3†). Therefore, the unusual chiral-source-concentration-dependent CPL property of **APy** was investigated. In the presence of 0.6 equiv. of chiral **1**, CPL activity with emission maxima consistent with those in the fluorescence spectra were observed (Fig. 6). The $|g_{lum}|$ value reached approx. 1.7×10^{-3} at 550 nm (Fig. S37†). To our knowledge, this is the highest g_{lum} value reported to date for pillar[*n*]arene-containing systems capable of CPL properties in solution.[17a,c] Furthermore, further feeding with the chiral source eliminated the CPL of **APy** owing to decreased CD induction and emission, indicating that CPL on/off control was achieved by continuous addition of planar chiral pillar[5]arenes.

Conclusions

In conclusion, we synthesized cationic water-soluble planar-chiral pillar[5]arenes *S*-**1** and *R*-**1**, which were diastereomerically pure in water (*pR* for *S*-**1**, *pS* for *R*-**1**). Compared with simple chiral molecules (such as *R*-**unit** and L-**Val**), planar chiral pillar[5]arene **1** readily transferred chiral information to guest molecule **APy** through host–guest interactions. Interestingly, the chirality transfer efficiency and subsequent CPL properties were sensitive to the host–guest feed ratio owing to the bulkiness of planar chiral macrocycle **1**. Adding a small amount of **1** (0.6 equiv.) resulted in CPL of **APy**. The strategy of using readily obtained chiral macrocyclic molecules as the chiral source makes the chirality transfer process more diverse and interesting, and can be finely regulated, which might provide new possibilities in the area of supramolecular CPL materials. In particular, planar chiral pillar[5]arenes strongly bound the linear aliphatic chains of fluorescent guest molecules, with only a minor impact on the physical properties of the fluorophores. However, complexation of linear aliphatic chains in the supramolecular assemblies of **Apy** resulted in effective chiral transmission from planar chiral pillar[5]arenes to the fluorescent guest molecules. Various fluorescent supramolecular assemblies composed of linear aliphatic chains and fluorophore(s)

have been reported,[32] so whether pillar[5]arenes **1** can transfer chiral information to them should be investigated. This is currently under investigation in our group.

Data availability

All analytical data is provided in the narrative and in the ESI.†

Author contributions

S. F. and T. O.: conceptualization, methodology, formal analysis, investigation, writing-original draft and editing. T. O.: project administration, funding acquisition and supervision. S. F., S. O., K. K.: resources and validation. T. T., K. W., K. Y., M. G., K. T., T. K., T. Y.: formal analysis and resources.

Conflicts of interest

There are no conflicts to declare.

Acknowledgements

This work was supported by JSPS KAKENHI Grant Numbers JP15H00990, JP17H05148, JP18H04510, and JP20H04670 (Scientific Research on Innovative Areas, T. O.), JP19H00909 (Scientific Research (A), T. O.), JP21K14612 (Early-Career Scientists, S. F.), JP20K22528 (Research Activity Start-up, K. K.) and JP21K14611 (Early-Career Scientists, K.K.), JST CREST Grant Number JPMJCR18R3 (T. O.), the Nanotechnology Platform Program of the Ministry of Education, Culture, Sports, Science and Technology (MEXT), and MEXT World Premier International Research Center Initiative (WPI), Japan.

Notes and references

1 (*a*) J. R. Brandt, F. Salerno and M. J. Fuchter, *Nat. Rev. Chem.*, 2017, **1**, 0045; (*b*) D. Zhao, T. van Leeuwen, J. Cheng and B. L. Feringa, *Nat. Chem.*, 2017, **9**, 250–256; (*c*) C. Kulkarni, A. K. Mondal, T. K. Das, G. Grinbom, F. Tassinari, M. F. J. Mabesoone, E. W. Meijer and R. Naaman, *Adv. Mater.*, 2020, **32**, 1904965; (*d*) K. Shimomura, T. Ikai, S. Kanoh, E. Yashima and K. Maeda, *Nat. Chem.*, 2014, **6**, 429–434; (*e*) P. Duan, H. Cao, L. Zhang and M. Liu, *Soft Matter*, 2014, **10**, 5428–5448.

2 (*a*) F. Zinna and L. Di Bari, *Chirality*, 2015, **27**, 1–13; (*b*) H. Maeda, Y. Bando, K. Shimomura, I. Yamada, M. Naito, K. Nobusawa, H. Tsumatori and T. Kawai, *J. Am. Chem. Soc.*, 2011, **133**, 9266–9269; (*c*) Y. Zhao, N. A. A. Rahirn, Y. Xia, M. Fujiki, B. Song, Z. Zhang, W. Zhang and X. Zhu, *Macromolecules*, 2016, **49**, 3214–3221.

3 (*a*) M. Grell, M. Oda, K. S. Whitehead, A. Asimakis, D. Neher and D. D. C. Bradley, *Adv. Mater.*, 2001, **13**, 577–580; (*b*) Y. Geng, A. Trajkovska, S. W. Culligan, J. J. Ou, H. M. P. Chen, D. Katsis and S. H. Chen, *J. Am. Chem. Soc.*, 2003, **125**, 14032–14038; (*c*) M. Li, S.-H. Li, D. Zhang, M. Cai, L. Duan, M.-K. Fung and C.-F. Chen, *Angew. Chem., Int. Ed.*, 2018, **57**, 2889–2893; (*d*) M. Sun, L. Xu, A. Qu, P. Zhao, T. Hao, W. Ma, C. Hao, X. Wen, F. M. Colombari, A. F. de Moura, N. A. Kotov, C. Xu and H. Kuang, *Nat. Chem.*, 2018, **10**, 821–830.

4 (*a*) H. K. Bisoyi and Q. Li, *Angew. Chem., Int. Ed.*, 2016, **55**, 2994–3010; (*b*) Y. Kim, B. Yeom, O. Arteaga, S. J. Yoo, S. G. Lee, J. G. Kim and N. A. Kotov, *Nat. Mater.*, 2016, **15**, 461–468.

5 (*a*) M. Schadt, *Annu. Rev. Mater. Sci.*, 1997, **27**, 305–379; (*b*) M. C. Heffern, L. M. Matosziuk and T. J. Meade, *Chem. Rev.*, 2014, **114**, 4496–4539; (*c*) J. Han, S. Guo, H. Lu, S. Liu, Q. Zhao and W. Huang, *Adv. Opt. Mater.*, 2018, **6**, 1800538.

6 (*a*) E. M. Sánchez-Carnerero, A. R. Agarrabeitia, F. Moreno, B. L. Maroto, G. Muller, M. J. Ortiz and S. de la Moya, *Chem.–Eur. J.*, 2015, **21**, 13488–13500; (*b*) J. F. Koegel, S. Kusaka, R. Sakamoto, T. Iwashima, M. Tsuchiya, R. Toyoda, R. Matsuoka, T. Tsukamoto, J. Yuasa, Y. Kitagawa, T. Kawai and H. Nishihara, *Angew. Chem., Int. Ed.*, 2016, **55**, 1377–1381; (*c*) K. Takaishi, K. Iwachido, R. Takehana, M. Uchiyama and T. Ema, *J. Am. Chem. Soc.*, 2019, **141**, 6185–6190; (*d*) Z.-B. Sun, J.-K. Liu, D.-F. Yuan, Z.-H. Zhao, X.-Z. Zhu, D.-H. Liu, Q. Peng and C.-H. Zhao, *Angew. Chem., Int. Ed.*, 2019, **58**, 4840–4846; (*e*) Y. Saito, M. Satake, R. Mori, M. Okayasu, H. Masu, M. Tominaga, K. Katagiri, K. Yamaguchi, S. Kikkawa, H. Hikawa and I. Azumaya, *Org. Biomol. Chem.*, 2020, **18**, 230–236; (*f*) K. Nakamura, S. Furumi, M. Takeuchi, T. Shibuya and K. Tanaka, *J. Am. Chem. Soc.*, 2014, **136**, 5555–5558; (*g*) J. Zhu, S. Chen and C. He, *J. Am. Chem. Soc.*, 2021, **143**, 5301–5307.

7 (*a*) M. Oda, H. G. Nothofer, G. Lieser, U. Scherf, S. C. J. Meskers and D. Neher, *Adv. Mater.*, 2000, **12**, 362–365; (*b*) S.-T. Wu, Z.-W. Cai, Q.-Y. Ye, C.-H. Weng, X.-H. Huang, X.-L. Hu, C.-C. Huang and N.-F. Zhuang, *Angew. Chem., Int. Ed.*, 2014, **53**, 12860–12864; (*c*) B. A. San Jose, J. L. Yan and K. Akagi, *Angew. Chem., Int. Ed.*, 2014, **53**, 10641–10644; (*d*) S. T. Duong and M. Fujiki, *Polym. Chem.*, 2017, **8**, 4673–4679; (*e*) B. Zhao, X. Gao, K. Pan and J. Deng, *ACS Nano*, 2021, **15**, 7463–7471; (*f*) Y. Ru, L. Sui, H. Song, X. Liu, Z. Tang, S.-Q. Zang, B. Yang and S. Lu, *Angew. Chem., Int. Ed.*, 2021, **60**, 14091–14099.

8 (*a*) S. H. Chen, D. Katsis, A. W. Schmid, J. C. Mastrangelo, T. Tsutsui and T. N. Blanton, *Nature*, 1999, **397**, 506–508; (*b*) Q. Ye, D. Zhu, L. Xu, X. Lu and Q. Lu, *J. Mater. Chem. C*, 2016, **4**, 1497–1503; (*c*) C.-T. Yeung, K.-H. Yim, H.-Y. Wong, R. Pal, W.-S. Lo, S.-C. Yan, M. Y.-M. Wong, D. Yufit, D. E. Smiles, L. J. McCormick, S. J. Teat, D. K. Shuh, W.-T. Wong and G.-L. Law, *Nat. Commun.*, 2017, **8**, 1128; (*d*) R. Aoki, R. Toyoda, J. F. Kögel, R. Sakamoto, J. Kumar, Y. Kitagawa, K. Harano, T. Kawai and H. Nishihara, *J. Am. Chem. Soc.*, 2017, **139**, 16024–16027; (*e*) X.-M. Chen, Y. Chen, L. Liang, Q.-J. Liu and Y. Liu, *Macromol. Rapid Commun.*, 2018, **39**, 1700869; (*f*) Y. Shi, G. Q. Yin, Z. Yan, P. Sang, M. Wang, R. Brzozowski, P. Eswara, L. Wojtas, Y. Zheng, X. Li and J. Cai, *J. Am. Chem. Soc.*, 2019, **141**, 12697–12706; (*g*) T. Zhao, J. Han, X. Jin, Y. Liu, M. Liu and P. Duan, *Angew. Chem., Int. Ed.*, 2019, **58**, 4978–4982; (*h*)

H.-T. Feng, C. Liu, Q. Li, H. Zhang, J. W. Y. Lam and B. Z. Tang, *ACS Mater. Lett.*, 2019, **1**, 192–202.

9 (*a*) J.-L. Ma, Q. Peng and C.-H. Zhao, *Chem.–Eur. J.*, 2019, **25**, 15441–15454; (*b*) F. Song, Z. Zhao, Z. Liu, J. W. Y. Lam and B. Z. Tang, *J. Mater. Chem. C*, 2020, **8**, 3284–3301; (*c*) S. Wang, D. Hu, X. Guan, S. Cai, G. Shi, Z. Shuai, J. Zhang, Q. Peng and X. Wan, *Angew. Chem., Int. Ed.*, 2021, **60**, 21918–21926.

10 (*a*) K. Nakabayashi, T. Amako, N. Tajima, M. Fujiki and Y. Imai, *Chem. Commun.*, 2014, **50**, 13228–13230; (*b*) Y. Hashimoto, T. Nakashima, D. Shimizu and T. Kawai, *Chem. Commun.*, 2016, **52**, 5171–5174; (*c*) X. Bai, Y. Jiang, G. Zhao, J. Jiang, C. Yuan and M. Liu, *Soft Matter*, 2021, **17**, 4328–4334; (*d*) T. Ikai, Y. Wada, S. Awata, C. Yun, K. Maeda, M. Mizuno and T. M. Swager, *Org. Biomol. Chem.*, 2017, **15**, 8440–8447; (*e*) A. Homberg, E. Brun, F. Zinna, S. Pascal, M. Górecki, L. Monnier, C. Besnard, G. Pescitelli, L. Di Bari and J. Lacour, *Chem. Sci.*, 2018, **9**, 7043–7052; (*f*) Y. Imai and J. Yuasa, *Chem. Commun.*, 2019, **55**, 4095–4098.

11 (*a*) K. Maeda, M. Nozaki, K. Hashimoto, K. Shimomura, D. Hirose, T. Nishimura, G. Watanabe and E. Yashima, *J. Am. Chem. Soc.*, 2020, **142**, 7668–7682; (*b*) T. Goto, Y. Okazaki, M. Ueki, Y. Kuwahara, M. Takafuji, R. Oda and H. Ihara, *Angew. Chem., Int. Ed.*, 2017, **56**, 2989–2993; (*c*) Z. Shen, T. Wang, L. Shi, Z. Tang and M. Liu, *Chem. Sci.*, 2015, **6**, 4267–4272; (*d*) J. Han, J. You, X. Li, P. Duan and M. Liu, *Adv. Mater.*, 2017, **29**, 1606503; (*e*) A. H. G. David, R. Casares, J. M. Cuerva, A. G. CampaÇa and V. Blanco, *J. Am. Chem. Soc.*, 2019, **141**, 18064–18074; (*f*) Q. Jiang, X. Xu, P.-A. Yin, K. Ma, Y. Zhen, P. Duan, Q. Peng, W.-Q. Chen and B. Ding, *J. Am. Chem. Soc.*, 2019, **141**, 9490–9494; (*g*) Y. Li, Q. Li, X. Miao, C. Qin, D. Chu and L. Cao, *Angew. Chem., Int. Ed.*, 2021, **60**, 6744–6951.

12 (*a*) A. Szumna, *Chem. Soc. Rev.*, 2010, **39**, 4274–4285; (*b*) Y. Shoji, K. Tashiro and T. Aida, *J. Am. Chem. Soc.*, 2006, **128**, 10690–10691; (*c*) G.-W. Zhang, P.-F. Li, Z. Meng, H.-X. Wang, Y. Han and C.-F. Chen, *Angew. Chem., Int. Ed.*, 2016, **55**, 5304–5308; (*d*) S. Tong, J.-T. Li, D.-D. Liang, Y.-E. Zhang, Q.-Y. Feng, X. Zhang, J. Zhu and M.-X. Wang, *J. Am. Chem. Soc.*, 2020, **142**, 14432–14436; (*e*) H. Chai, Z. Chen, S.-H. Wang, M. Quan, L.-P. Yang, H. Ke and W. Jiang, *CCS Chem.*, 2020, **2**, 440–452; (*f*) R. Ning, H. Zhu, S.-X. Nie, Y.-F. Ao, D.-X. Wang and Q.-Q. Wang, *Angew. Chem., Int. Ed.*, 2020, **59**, 10894–10898; (*g*) T. Miura, T. Nakamura, Y. Ishihara, Y. Nagata and M. Murakami, *Angew. Chem., Int. Ed.*, 2020, **59**, 20475–20479; (*h*) N. Luo, Y.-F. Ao, D.-X. Wang and Q.-Q. Wang, *Angew. Chem., Int. Ed.*, 2021, **60**, 20650–20655; (*i*) X.-N. Han, Y. Han and C.-F. Chen, *J. Am. Chem. Soc.*, 2020, **142**, 8262–8269.

13 J. Li, H.-Y. Zhou, Y. Han and C.-F. Chen, *Angew. Chem., Int. Ed.*, 2021, **60**, 21927–21933.

14 (*a*) M. Inouye, K. Hayashi, Y. Yonenaga, T. Itou, K. Fujimoto, T.-a. Uchida, M. Iwamura and K. Nozaki, *Angew. Chem., Int. Ed.*, 2014, **53**, 14392–14396; (*b*) Y. Zhang, D. Yang, J. Han, J. Zhou, Q. Jin, M. Liu and P. Duan, *Langmuir*, 2018, **34**, 5821–5830; (*c*) C. Yang, W. Chen, X. Zhu, X. Song and M. Liu, *J. Phys. Chem. Lett.*, 2021, **12**, 7491–7496; (*d*) K. Hayashi, Y. Miyaoka, Y. Ohishi, T.-a. Uchida, M. Iwamura, K. Nozaki and M. Inouye, *Chem.–Eur. J.*, 2018, **24**, 14613–14616.

15 (*a*) T. Ogoshi, S. Kanai, S. Fujinami, T. Yamagishi and Y. Nakamoto, *J. Am. Chem. Soc.*, 2008, **130**, 5022–5023; (*b*) M. Xue, Y. Yang, X. Chi, Z. Zhang and F. Huang, *Acc. Chem. Res.*, 2012, **45**, 1294–1308; (*c*) N. L. Strutt, H. Zhang, S. T. Schneebeli and J. F. Stoddart, *Acc. Chem. Res.*, 2014, **47**, 2631–2642; (*d*) T. Ogoshi, T. Yamagishi and Y. Nakamoto, *Chem. Rev.*, 2016, **116**, 7937–8002; (*e*) S. Fa, T. Kakuta, T. Yamagishi and T. Ogoshi, *CCS Chem.*, 2019, **1**, 50–63; (*f*) E. Li, K. Jie, M. Liu, X. Sheng, W. Zhu and F. Huang, *Chem. Soc. Rev.*, 2020, **49**, 1517–1544; (*g*) Z. Li and Y.-W. Yang, *Acc. Mater. Res.*, 2021, **2**, 292–305; (*h*) K. Kato, S. Ohtani, S. Fa and T. Ogoshi, *Bull. Chem. Soc. Jpn.*, 2021, **94**, 2319–2328.

16 (*a*) S. Fa, T. Kakuta, T. Yamagishi and T. Ogoshi, *Chem. Lett.*, 2019, **48**, 1278–1287; (*b*) J.-F. Chen, J.-D. Ding and T.-B. Wei, *Chem. Commun.*, 2021, **57**, 9029–9039.

17 (*a*) J.-F. Chen, X. Yin, B. Wang, K. Zhang, G. Meng, S. Zhang, Y. Shi, N. Wang, S. Wang and P. Chen, *Angew. Chem., Int. Ed.*, 2020, **59**, 11267–11272; (*b*) W.-J. Li, Q. Gu, X.-Q. Wang, D.-Y. Zhang, Y.-T. Wang, X. He, W. Wang and H.-B. Yang, *Angew. Chem., Int. Ed.*, 2021, **60**, 9507–9515; (*c*) J.-F. Chen, X. Yin, K. Zhang, Z. Zhao, S. Zhang, N. Zhang, N. Wang and P. Chen, *J. Org. Chem.*, 2021, **86**, 12654–12663; (*d*) H. Zhu, Q. Li, B. Shi, H. Xing, Y. Sun, S. Lu, L. Shangguan, X. Li, F. Huang and P. J. Stang, *J. Am. Chem. Soc.*, 2020, **142**, 17340–17345.

18 (*a*) T. Ogoshi, K. Kitajima, T. Aoki, S. Fujinami, T. Yamagishi and Y. Nakamoto, *J. Org. Chem.*, 2010, **75**, 3268–3273; (*b*) H. Zhu, Q. Li, Z. Gao, H. Wang, B. Shi, Y. Wu, L. Shangguan, X. Hong, F. Wang and F. Huang, *Angew. Chem., Int. Ed.*, 2020, **59**, 10868–10872; (*c*) Y. Chen, L. Fu, B. Sun, C. Qian, R. Wang, J. Jiang, C. Lin, J. Ma and L. Wang, *Org. Lett.*, 2020, **22**, 2266–2270; (*d*) J. Ji, Y. Li, C. Xiao, G. Cheng, K. Luo, Q. Gong, D. Zhou, J. J. Chruma, W. Wu and C. Yang, *Chem. Commun.*, 2020, **56**, 161–164; (*e*) K. Du, P. Demay-Drouhard, K. Samanta, S. Li, T. U. Thikekar, H. Wang, M. Guo, B. van Lagen, H. Zuihof and A. C.-H. Sue, *J. Org. Chem.*, 2020, **85**, 11368–11374; (*f*) S. Fa, K. Egami, K. Adachi, K. Kato and T. Ogoshi, *Angew. Chem., Int. Ed.*, 2020, **59**, 20353–20356.

19 (*a*) T. F. Al-Azemi, M. Vinodh, F. H. Alipour and A. A. Mohamod, *RSC Adv.*, 2019, **9**, 23295–23301; (*b*) N. L. Strutt, H. Zhang and J. F. Stoddart, *Chem. Commun.*, 2014, **50**, 7455–7458; (*c*) T. Ogoshi, K. Masaki, R. Shiga, K. Kitajima and T. Yamagishi, *Org. Lett.*, 2011, **13**, 1264–1266; (*d*) T. Ogoshi, R. Shiga, M. Hashizume and T. Yamagishi, *Chem. Commun.*, 2011, **47**, 6927–6929; (*e*) Q. Li, X. Li, L. Ning, C.-H. Tan, Y. Mu and R. Wang, *Small*, 2019, **15**, 1804678; (*f*) S. Fa, M. Mizobata, S. Nagano, K. Suetsugu, T. Kakuta, T. Yamagishi and T. Ogoshi, *ACS Nano*, 2021, **15**, 16794–16801.

20 (*a*) Y. Nagata, M. Suzuki, Y. Shimada, H. Sengoku, S. Nishida, T. Kakuta, T. Yamagishi, M. Suginome and T. Ogoshi, *Chem.*

Commun., 2020, **56**, 8424–8427; (*b*) T. Ogoshi, R. Shiga, T. Yamagishi and Y. Nakamoto, *J. Org. Chem.*, 2011, **76**, 618–622.

21 T. Ogoshi, K. Umeda, T. Yamagishi and Y. Nakamoto, *Chem. Commun.*, 2009, **45**, 4874–4876.

22 J. Yao, W. Wu, W. Liang, Y. Feng, D. Zhou, J. J. Chruma, G. Fukuhara, T. Mori, Y. Inoue and C. Yang, *Angew. Chem., Int. Ed.*, 2017, **56**, 6869–6873.

23 S. Fa, K. Adachi, K. Egami, K. Kato and T. Ogoshi, *Chem. Sci.*, 2021, **12**, 3483–3488.

24 One set of signals was also observed in other protic solvents such as methanol-d_4. Details were shown in the ESI.†

25 J. Park, Y. Choi, S. S. Lee and J. H. Jung, *Org. Lett.*, 2019, **21**, 1232–1236.

26 Although the *g* value of *S*-**1** in water was smaller than those enantio-pure examples, a high value was reached after complexation with guests due to stop of the unit swing.

27 (*a*) X. Hu, H. Deng, J. Li, X. Jia and C. Li, *Chin. Chem. Lett.*, 2013, **24**, 707–709; (*b*) X. Shu, S. Chen, J. Li, Z. Chen, L. Weng, X. Jia and C. Li, *Chem. Commun.*, 2012, **48**, 2967–2969.

28 Y. Ma, M. Xue, Z. Zhang, X. Chi and F. Huang, *Tetrahedron*, 2013, **69**, 4532–4535.

29 K. Han, Y. Zhang, J. Li, Y. Yu, X. Jia and C. Li, *Eur. J. Org. Chem.*, 2013, **2013**, 2057–2060.

30 (*a*) H. Anetai, Y. Wada, T. Takeda, N. Hoshino, S. Yamamoto, M. Mitsuishi, T. Takenobu and T. Akutagawa, *J. Phys. Chem. Lett.*, 2015, **6**, 1813–1818; (*b*) Y.-Y. Chen, H. Wang, D.-W. Zhang, J.-L. Hou and Z.-T. Li, *Chem. Commun.*, 2015, **51**, 12088–12091; (*c*) Y. Ohishi and M. Inouye, *Tetrahedron Lett.*, 2019, **60**, 151232.

31 At low concentration, the fluorescence maximum was clearly observed at *ca.* 426 nm, corresponding to the emission of monomeric **APy**. As concentration increased, a new fluorescence band emerged at *ca.* 530 nm and gradually red-shift, indicating the formation of the π-oligomer of **APy**. For detailed discussion, see the ESI.†

32 (*a*) J. Zhao and P. Xing, *ChemPlusChem*, 2020, **85**, 1511–1522; (*b*) J. Zhao and P. Xing, *ChemPhotoChem*, 2022, **6**, e202100124.